Numerical Studies of Multicomponent Chromatography Using pH Gradients

Douglas D. Frey, Andrew Barnes, and John Strong
Dept. of Chemical and Biochemical Engineering, University of Maryland Baltimore County, Baltimore, MD 21228

A general numerical method is developed for multicomponent chromatography for the case where a pH gradient occurs and several buffering species are present that become adsorbed together with the components being separated through an ion-exchange mechanism. Acid-base equilibrium relations are used to determine the ionic compositions in the liquid and adsorbed phases and are solved using a single-variable Newton's method. The differential material-balance relations are integrated numerically using the method of characteristics. The transport relations are incorporated using a matrix analog of the linear-driving-force approximation. The resulting method accounts for the adsorption of each ionic form of each buffering species, for multicomponent diffusional interactions arising from induced electric fields, for volume and concentration overloading of proteins, and for changes in the adsorption capacity caused by pH variations. Numerical calculations illustrate factors governing the selection of the adsorbent and buffer components for use in separating mixtures of proteins using retained, internally generated pH gradients.

Introduction

A number of workers have developed methods for determining the adsorption dynamics of ion-exchange chromatography where several buffering species are employed that become adsorbed together with the components being separated. However, these previous methods all contain approximations that limit their ability to predict detailed behavior. For example, the methods of Helfferich and Bennett (1984a,b) and Klein et al. (1982) apply to local-equilibrium behavior as well as to Langmuir isotherms and Riemann boundary conditions. Similarly, the methods of Sluyterman and Elgersma (1978) and Murel et al. (1985, 1986) use empirical heights of an equilibrium stage, rather than the actual transport relations, as well as approximations for determining the liquid-phase pH. Finally, none of these methods are able to determine the effluent concentration profile for a protein introduced as a feed slug into a chromatography column.

In contrast to this previous work, this study accounts quantitatively for the various phenomena that occur, including the diffusional processes in the particle pores and the acid-base equilibrium relations in the liquid and adsorbed phases. With such a model, rational strategies can be developed for selecting operating conditions, adsorbents, and buffer compositions in chromatographic processes where pH gradients occur. Of special interest in this regard is the process of chromatofocusing where a column is presaturated with a buffer at one pH, and elution is carried out with an instantaneous change from the presaturation buffer to an eluent containing a mixture of buffering species at another pH. This results in an internally generated, gradual pH gradient in the column effluent (as opposed to a pH gradient generated by external mixing) that can be used in protein separations (Scopes, 1987).

The work described here is related to the studies of Engasser and Horváth (1974) and of Saville and Palusinski (1986), who investigated the effect of pH in bound enzyme systems and in electrophoresis, respectively. This work is also related to the study of Saunders et al. (1989), who investigated the chromatography of amino acids, and to the study of Berninger et al. (1991), who investigated chromatography in reacting systems. In this work, however, several simplifications and extensions are employed so that numerical calculations involving large numbers of components can be performed efficiently. In particular, there are no assumptions made concerning which ionic forms of a particular buffering species are present, and all species, including the ionizable

Correspondence concerning this article should be addressed to D. D. Frey.
Current address of A. Barnes: Dept. of Mathematics, Duke University, Durham, NC 27706.

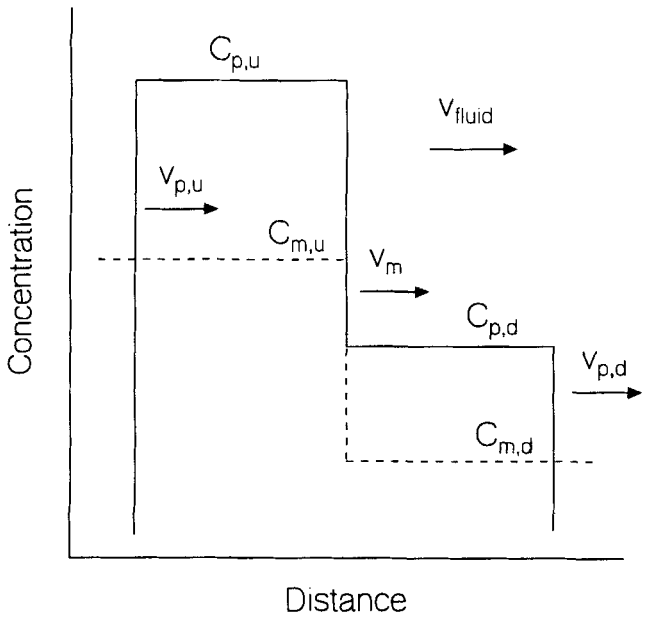

Figure 1. Solute band overtaken by a change in solvent modifier composition.

functional groups attached to the adsorbent, are treated in an identical manner, which facilitates model development. In addition, the transport relations are incorporated using efficient matrix approximations and the material-balance relations are integrated using the method of characteristics with a variable step size. Finally, the methods developed here account for variations in adsorption capacity caused by the effect of pH on weakly acidic or basic functional groups attached to the adsorbent.

Although the main purpose of this study is to develop a general numerical method for ion-exchange chromatography employing pH gradients, it has three additional objectives: (1) to compare numerical calculations with experimental data obtained in this study and in previous studies by other workers; (2) to use numerical calculations to illustrate factors governing the selection of adsorbent-buffer systems for producing gradients in pH and total ionic concentration; and (3) to use numerical calculations to investigate the behavior underlying protein separations in chromatography columns when internally generated pH gradients are employed.

Migration of Solute Bands: Basic Concepts

Figure 1 illustrates axial composition profiles in a chromatography column under local-equilibrium conditions when a step change in the concentration of a solvent component, termed here the solvent modifier, overtakes a solute band and causes a change in the adsorption equilibrium constant for the solute. For simplicity, linear equilibrium is assumed so that the upstream and downstream sides of the solute band remain as abrupt steps. Under these conditions, a step change in concentration travels through the column with a velocity given by (Wankat, 1986, 1990)

$$v_{\Delta C} = \frac{v_{\text{fluid}}}{1 + (\rho_b/\alpha)(\Delta q_i/\Delta C_i)}. \tag{1}$$

If Eq. 1 is written for both the solvent modifier and the solute, it follows that the change in solute concentration caused by its interaction with the solvent modifier is given by

$$\frac{C_{p,u}}{C_{p,d}} = \frac{v_{p,d}^{-1} - v_m^{-1}}{v_{p,u}^{-1} - v_m^{-1}} \tag{2}$$

where u and d denote conditions upstream and downstream of the step change in solvent modifier, p denotes the solute, and m denotes the solvent modifier.

Consider the case when v_m is equal to the velocity of an unadsorbed solute and is therefore much greater than either $v_{p,u}$ or $v_{p,d}$, which is approximately the situation in ion-exchange chromatography when a change in total ionic concentration is used to form a gradient. Equation 2 then yields $C_{p,u}/C_{p,d} = v_{p,u}/v_{p,d}$, which indicates that the change in solute concentration is determined by equilibrium behavior. Alternatively, when a pH change is used to form a gradient, it is possible for the velocity of the pH change to be significantly less than the velocity of an unadsorbed solute. In particular, if the criterion $v_{p,u} > v_m > v_{p,d}$ is satisfied, then Eq. 2 yields $C_{p,u}/C_{p,d} < 0$: the equilibrium model predicts an infinite solute concentration change so that mass-transfer resistances determine the band shape. When that occurs, any solute downstream from the step change in solvent modifier has a velocity less than the solvent modifier step and is eventually overtaken by the step. Conversely, any solute upstream from the solvent modifier step has a velocity greater than the step, and eventually overtakes it, so that all of the solute tends to be located at the step. When the change in solvent modifier is gradual, rather than stepwise, all of the solute collects analogously at the point on the gradient where $v_p = v_m$. In either case, a focusing effect occurs that has the potential of producing narrow solute bands.

Liquid-Phase Equilibria for Buffering Species

Consider a buffering species such as malic acid that has two ionizable functional groups and therefore three ionic forms. The acid-base dissociation reactions can be written as

$$A_i^+ \rightleftharpoons A_i^\circ + H^+ \tag{3}$$

$$A_i^\circ \rightleftharpoons A_i^- + H^+ \tag{4}$$

where A_i^-, A_i°, and A_i^+ denote the most negatively charged, the second most negatively charged, and the most positively charged individual ionic forms of the buffering species A_i. Equations 3 and 4 lead, respectively, to the following equilibrium relations:

$$K_{A_i,\text{fluid},1} = C_{A_i^\circ} C_{H^+}/C_{A_i^+} \tag{5}$$

$$K_{A_i,\text{fluid},2} = C_{A_i^-} C_{H^+}/C_{A_i^\circ}. \tag{6}$$

Substitutions using Eqs. 5 and 6 yield the following expressions for the amount of each individual ion present:

$$C_{A_i^+} = \frac{C_{A_i}}{1 + K_{A_i,\text{fluid},1}/C_{H^+} + K_{A_i,\text{fluid},1}K_{A_i,\text{fluid},2}/C_{H^+}^2} \quad (7)$$

$$C_{A_i^\circ} = \frac{K_{A_i,\text{fluid},1}C_{A_i}}{C_{H^+} + K_{A_i,\text{fluid},1} + K_{A_i,\text{fluid},1}K_{A_i,\text{fluid},2}/C_{H^+}} \quad (8)$$

$$C_{A_i^-} = \frac{C_{A_i}}{1 + C_{H^+}/K_{A_i,\text{fluid},2} + C_{H^+}^2/(K_{A_i,\text{fluid},1}K_{A_i,\text{fluid},2})}. \quad (9)$$

The electroneutrality condition in the liquid phase can be written

$$\sum_{i=1}^{N_A} (z_{A_i^+}C_{A_i^+} + z_{A_i^\circ}C_{A_i^\circ} + z_{A_i^-}C_{A_i^-}) + C_{H^+} - \frac{K_{w,\text{fluid}}}{C_{H^+}} = 0 \quad (10)$$

where $K_{w,\text{fluid}}$ is the liquid-phase dissociation constant for water. Substitution of Eqs. 7–9 into Eq. 10 yields

$$f(C_{H^+}) = 0 = \sum_{i=1}^{N_A} \left(C_{A_i} z_{A_i^\circ} + \frac{C_{A_i}(C_{H^+}^2 - K_{A_i,\text{fluid},1}K_{A_i,\text{fluid},2})}{C_{H^+}^2 + K_{A_i,\text{fluid},1}C_{H^+} + K_{A_i,\text{fluid},1}K_{A_i,\text{fluid},2}} \right) + C_{H^+} - \frac{K_{w,\text{fluid}}}{C_{H^+}}, \quad (11)$$

which can be solved for C_{H^+} using Newton's method. However, since $f(C_{H^+})$ is more nearly a linear function of $\ln(C_{H^+})$ (that is, of pH), rather than C_{H^+}, the efficiency of Newton's method can be increased by using logarithmic extrapolation according to the following recurrence relation:

$$\ln(C_{H^+})_{k+1} = \ln(C_{H^+})_k - \frac{f(C_{H^+})_k}{C_{H^+}(df(C_{H^+})/dC_{H^+})_k} \quad (12)$$

where k and $k+1$ denote consecutive iterates. The derivative $df(C_{H^+})/dC_{H^+}$ is given by

$$\frac{df(C_{H^+})}{dC_H^+} = \sum_{i=1}^{N_A} \left(C_{A_i} K_{A_i,\text{fluid},1} \frac{C_{H^+}^2 + 4K_{A_i,\text{fluid},2}C_{H^+} - K_{A_i,\text{fluid},1}K_{A_i,\text{fluid},2}}{\left(C_{H^+}^2 + K_{A_i,\text{fluid},1}C_{H^+} + K_{A_i,\text{fluid},1}K_{A_i,\text{fluid},2}\right)^2} \right) + 1 + \frac{K_{w,\text{fluid}}}{C_{H^+}^2}. \quad (13)$$

The hydrogen ion concentration determined in this way can be substituted into Eqs. 7–9 written for each buffering species to calculate the concentrations of all ions present in the liquid phase. Therefore, if the concentration of each buffering species (such as C_{A_i}) is given, then the amount of each individual ion (such as $C_{A_i^+}$) can be determined by solving iteratively a single equation for the unknown C_{H^+} and then substituting that value into Eqs. 7–9. Although Eqs. 11 and 13 assume that all buffering species have two ionizable functional groups, those equations can be modified to account for buffering species that have a single ionizable functional group, or which are strong electrolytes, by evaluating the appropriate equilibrium constants as either very large or very small to yield the desired behavior.

Under certain conditions the electroneutrality condition for the liquid phase (as well as certain other relations discussed below) can be solved analytically. For example, if only two monofunctional buffers are present, if the protein concentration is small enough so that the presence of proteins can be ignored in the electroneutrality condition, and if the presence of H^+ and OH^- ions are similarly ignored, then Eq. 11 reduces to a quadratic equation for C_{H^+}. In this study these types of simplified analytical relations will be not be utilized since the goal of this study is to develop a numerical method that can account for any number of buffering species, for high protein concentrations, and that can be readily modified to account for various nonidealities, such as composition-dependent equilibrium parameters.

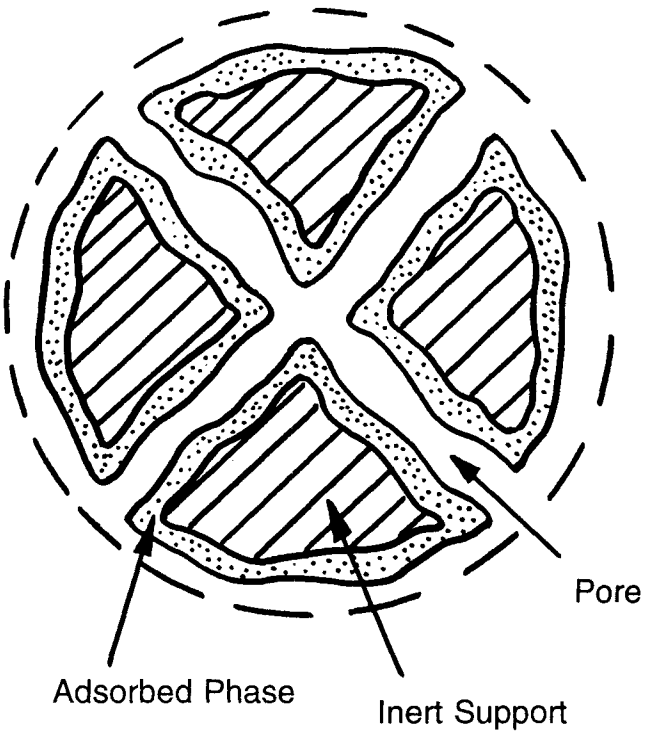

Figure 2. Structure of adsorbent particle.

Adsorbed-Phase Equilibria for Buffering Species

Figure 2 illustrates the three phases that constitute a typical adsorbent: (1) a phase containing the adsorbates; (2) the liquid-filled pores; and (3) an inert phase onto which the ad-

sorbate-containing phase is attached. The acid-base equilibrium relations that apply to the buffering species in the adsorbed phase, as well as the expressions for interphase equilibrium described in later sections, can be formulated by representing the adsorbed phase as a concentrated electrolyte solution with all species, including the functional groups attached to the adsorbent, uniformly distributed. Consider the case where each of the three phases shown in Figure 2 has a uniform composition and where one or more types of ionizable functional groups are attached to the adsorbent. Furthermore, so that the resulting equations can be put into a form identical to that in the preceding section, it is assumed that each functional group attached to the adsorbent can exist in three different ionic forms so that the following acid-base dissociation reactions apply:

$$R_i^+ \rightleftharpoons R_i^\circ + H^+ \tag{14}$$

$$R_i^\circ \rightleftharpoons R_i^- + H^+ \tag{15}$$

where R_i^-, R_i°, and R_i^+ denote the most negatively charged, the second most negatively charged, and the most positively charged forms of the functional group R_i.

Equilibrium relations identical to those given by Eqs. 5 and 6 apply to the buffering species present in the adsorbed phase and can be written

$$K_{A_i\text{ads},1} = q_{A_i^\circ,\text{ads}} q_{H^+,\text{ads}} / q_{A_i^+,\text{ads}} \tag{16}$$

$$K_{A_i\text{ads},2} = q_{A_i^-,\text{ads}} q_{H^+,\text{ads}} / q_{A_i^\circ,\text{ads}} \tag{17}$$

where the subscript ads denotes concentrations per unit volume of adsorbed phase. Equations 16 and 17 lead to the following relations:

$$q_{A_i^+,\text{ads}} = \frac{q_{A_i\text{ads}}}{1 + K_{A_i\text{ads},1}/q_{H^+,\text{ads}} + K_{A_i\text{ads},1} K_{A_i\text{ads},2}/q_{H^+,\text{ads}}^2} \tag{18}$$

$$q_{A_i^\circ,\text{ads}} = \frac{K_{A_i\text{ads},1} q_{A_i\text{ads}}}{q_{H^+,\text{ads}} + K_{A_i\text{ads},1} + K_{A_i\text{ads},1} K_{A_i\text{ads},2}/q_{H^+,\text{ads}}} \tag{19}$$

$$q_{A_i^-,\text{ads}} = \frac{q_{A_i\text{ads}}}{1 + q_{H^+,\text{ads}}/K_{A_i\text{ads},2} + q_{H^+}^2/(K_{A_i\text{ads},1} K_{A_i\text{ads},2})} \tag{20}$$

The electroneutrality condition in the adsorbed phase can be

$$\sum_{i=1}^{N_A} (z_{A_i^+} q_{A_i^+,\text{ads}} + z_{A_i^\circ} q_{A_i^\circ,\text{ads}} + z_{A_i^-} q_{A_i^-,\text{ads}}) + \sum_{i=1}^{N_R} (z_{R_i^+} q_{R_i^+} + z_{R_i^\circ} q_{R_i^\circ} + z_{R_i^-} q_{R_i^-}) + q_{H^+,\text{ads}} - \frac{K_{w,\text{sorbent}}}{q_{H^+,\text{ads}}} = 0. \tag{21}$$

By substituting Eqs. 18–20 written for each buffering species into Eq. 21, a relation of the form $g(q_{H^+,\text{ads}}) = 0$ can be developed and the quantity $q_{H^+,\text{ads}}$ solved for using Newton's method. The resulting equations are identical in form to Eqs. 11–13, but with the concentrations in the adsorbed phase replacing the liquid-phase concentrations and the summation extended to include the adsorbent functional groups. Therefore, as was the case for the liquid phase, if the total concentration of each buffering species (such as $q_{A_i,\text{ads}}$) is known, the individual ion concentrations (such as $q_{A_i^+,\text{ads}}$) can be determined by solving iteratively a single equation for $q_{H^+,\text{ads}}$ and then substituting that value into Eqs. 18–20.

The procedure just described yields the concentrations of each ion in a uniform adsorbed phase from the total amount of each buffering species in that phase. The total amount of a particular ion inside the adsorbent, however, also includes the unadsorbed ions in the particle pores. Although this contribution can be included in the calculation, the major reason for determining the individual ion concentrations in the particle is to use them in the matrix approximation for the mass-transfer rate described below. Therefore, it will usually be acceptable to ignore the unadsorbed ions in the particle pores when determining the individual ion concentrations in the particle. Furthermore, since the overall chromatographic behavior is largely determined by the strongly adsorbed ions, it will often be acceptable to ignore the unadsorbed ions in the particle pores throughout the entire calculation.

Interphase Equilibrium for Buffering Species

If the adsorbed phase is envisioned to be a homogeneous solution, and since at equilibrium the chemical potential of any electrically neutral combination of ions is the same in the adsorbed and extraparticle liquid phases, a set of equilibrium relations for these phases can be developed which, for the particular ionic species A_i^-, can be written

$$(q_{H^+,\text{ads}})^{-z_{A_i^-}} q_{A_i^-,\text{ads}} = K_{A_i^-,\text{ads}} (C_{H^+})^{-z_{A_i^-}} C_{A_i^-}. \tag{22}$$

Note that H^+ is used to form the electrically neutral ion combination since it is always present in both phases. In Eq. 22, $K_{A_i^-,\text{ads}}$ is an equilibrium parameter that may be a function of the adsorbed phase composition since it accounts for thermodynamic nonideality and the osmotic pressure difference between the adsorbed and extraparticle liquid phases. If Eq. 22 is written for the ions A_i^- and A_j^-, the results can be combined to yield a relation describing stoichiometric ion exchange:

$$K_{A_j^-A_i^-,\text{ads}} \equiv \left(\frac{q_{A_j^-,\text{ads}}}{C_{A_j^-}}\right)^{z_{A_i^-}} \Bigg/ \left(\frac{q_{A_i^-,\text{ads}}}{C_{A_i^-}}\right)^{z_{A_j^-}} = \left[\frac{K_{A_j\text{ads}}^{z_{A_i^-}}}{K_{A_i\text{ads}}^{z_{A_j^-}}}\right] \tag{23}$$

where $K_{A_j^-A_i^-,\text{ads}}$ is the ion-exchange equilibrium constant.

If the extraparticle liquid-phase composition is specified, then the electroneutrality condition in the adsorbed phase (Eq. 21) can be written in the form $h(q_{H^+,\text{ads}}) = 0$ by solving Eq. 22 written for each ionic form of each buffering species for the concentration of that ion in the adsorbent, and then substituting those quantities into Eq. 21 along with Eqs. 18–20 written for the adsorbent functional groups. This equation can then be solved for $q_{H^+,\text{ads}}$ using Newton's method in which case, if the adsorption equilibrium parameters (such as $K_{A_i^-,\text{ads}}$) are not functions of composition, the following relation can be used to determine $dh(q_{H^+,\text{ads}})/dq_{H^+,\text{ads}}$:

$$\frac{dh(q_{H^+,\text{ads}})}{dq_{H^+,\text{ads}}} = \sum_{i=1}^{N_A}\left(\frac{z_{A_i^+}^2 q_{A_i^+,\text{ads}}}{q_{H^+,\text{ads}}} + \frac{z_{A_i^0}^2 q_{A_i^0,\text{ads}}}{q_{H^+,\text{ads}}} + \frac{z_{A_i^-}^2 q_{A_i^-,\text{ads}}}{q_{H^+,\text{ads}}}\right) + 1 + \frac{K_{w,\text{sorbent}}}{q_{H^+,\text{ads}}^2} + \sum_{i=1}^{N_R}\left(q_{R_i} K_{R_{i1}} \frac{q_{H^+,\text{ads}}^2 + 4K_{R_{i2}} q_{H^+,\text{ads}} - K_{R_{i1}} K_{R_{i2}}}{\left(q_{H^+,\text{ads}}^2 + K_{R_{i1}} q_{H^+,\text{ads}}^2 + K_{R_{i1}} K_{R_{i2}}\right)^2}\right). \tag{24}$$

When the adsorption equilibrium parameters are functions of the adsorbed phase composition, then Eq. 24 can still be employed to determine $q_{H^+,\text{ads}}$ using Newton's method by evaluating the functions $q_{A_i^+,\text{ads}}(K_{A_i^+,\text{ads}}, q_{H^+,\text{ads}}, C_{H^+}, C_{A_i^+})$, $q_{A_i^0,\text{ads}}(K_{A_i^0,\text{ads}}, q_{H^+,\text{ads}}, C_{H^+}, C_{A_i^0})$, and $q_{A_i^-,\text{ads}}(K_{A_i^-,\text{ads}}, q_{H^+,\text{ads}}, C_{H^+}, C_{A_i^-})$ at the current iteration using the adsorbed phase composition from the previous iteration. The total amount of buffering species in the particle includes the unadsorbed material in the pores according to

$$q_{A_i} = \beta q_{A_i,\text{ads}} + \epsilon C_{A_i} \tag{25}$$

where β and ϵ are the volume fractions occupied by the adsorbed phase and by the pores, respectively, in the particle.

The equilibrium parameters just described for a particular buffering species are not independent. Instead, the definitions of these quantities imply that

$$K_{A_i,\text{ads},1} = K_{A_i,\text{fluid},1}\frac{K_{A_i^0,\text{ads}}}{K_{A_i^+,\text{ads}}} \tag{26}$$

with similar relations applying to the second ionization equilibrium for A_i. In general, the liquid-phase, acid-base equilibrium parameters are known, and the adsorption equilibrium parameters are fitted to experimental data. Acid-base equilibrium parameters in the adsorbed phase can then be calculated from Eq. 26. Note that if the adsorption equilibrium parameters are functions of composition, adsorbed-phase, acid-base equilibrium parameters are also functions of composition, and a modification of Newton's method similar to that just described must be used when solving the relations describing acid-base equilibrium in the adsorbed phase.

Incorporation of Proteins into the Liquid- and Adsorbed-Phase Acid-Base Equilibrium Expression

To incorporate proteins into the electroneutrality condition, the effective net charge as determined by acid-base titrimetry is needed as a function of pH (Tanford, 1960). Over a limited range, this charge can be approximated by a polynomial in pH such as

$$z_{P_i,\text{fluid}} = z_{i,\text{ref,fluid}} + a_{i,\text{fluid}}(\text{pH}_{i,\text{ref,fluid}} - \text{pH}_{\text{fluid}}) + b_{i,\text{fluid}}(\text{pH}_{i,\text{ref,fluid}} - \text{pH}_{\text{fluid}})^2 \tag{27}$$

The electroneutrality condition for the liquid phase, Eq. 10, can be modified by adding to the left side of that equation the quantity $z_{P_i,\text{fluid}}C_{P_i}$ summed over all the proteins. If Eq. 27 is employed, the derivative $df(C_{H^+})/dC_{H^+}$ needed in the solution of Eq. 11 by Newton's method is given by Eq. 13, but with the following term added to the right side:

$$\sum_{i=1}^{N_P}\{a_{i,\text{fluid}} + 2b_{i,\text{fluid}}[\text{pH}_{i,\text{ref,fluid}} + \log_{10}(C_{H^+})]\}\frac{C_{P_i}}{C_{H^+}\ln(10)}. \tag{28}$$

A similar approach can be used to incorporate the protein charge into the adsorbed-phase electroneutrality expression by assuming that Eq. 27 also applies to the adsorbed proteins. The extent to which this is true is generally unknown, in which case if Eq. 27 is used for both the liquid and adsorbed phases, the parameters in that equation should be considered as empirical constants that yield the best fit to experimental data.

Incorporation of Proteins into the Interphase Equilibrium Expressions

The representation of the adsorbed phase as a homogeneous electrolyte mixture is probably less applicable when the adsorbate is a macromolecular ion such as a protein than when the adsorbate is a small ion. In addition, a rigorous description of protein adsorption should account for the multiple charged states that exist for a protein and for the pH difference between the liquid and adsorbed phases. For simplicity, this study ignores these complications and instead follows the usual practice of employing a single empirical charge to describe the ability of each protein to displace buffer ions in the adsorbed phase. Therefore, as was the case for the buffering species, protein adsorption equilibrium can be expressed by equating the chemical potential of electrically neutral combinations of ions to yield

$$(q_{H^+})^{-z_{P_i,ix}} q_{P_i,\text{ads}} = K_{P_i,\text{ads}}(C_{H^+})^{-z_{P_i,ix}} C_{P_i} \tag{29}$$

where, over a limited range, the characteristic protein charge can again be approximated by a polynomial in pH such as

$$z_{P_i,ix} = z_{i,\text{ref},ix} + a_{i,ix}(\text{pH}_{i,\text{ref},ix} - \text{pH}_{\text{fluid}}) + b_{i,ix}(\text{pH}_{i,\text{ref},ix} - \text{pH}_{\text{fluid}})^2 \tag{30}$$

Equations 22 and 29 can also be combined to yield an expression describing stoichiometric ion exchange:

$$\left(\frac{q_{A_j^-,\text{ads}}}{C_{A_j^-}}\right)^{z_{P_i,ix}} = \left(\frac{K_{A_j^-,\text{ads}}^{z_{P_i,ix}}}{K_{P_i,\text{ads}}^{z_{A_j^-}}}\right)\left(\frac{q_{P_i,\text{ads}}}{C_{P_i}}\right)^{z_{A_j^-}} \tag{31}$$

Normally, the characteristic charge for the ion exchange of a protein is smaller than its charge determined by acid-base titrimetry, since only a portion of the net protein charge interacts with the adsorbent surface. Over a sufficiently small pH range, a linear relation between the characteristic charge and pH can be assumed with typical values for $a_{i,ix}$ varying from 0.5 to 2.5 pH^{-1} (Hearn et al., 1987).

The equilibrium amount of protein adsorbed can be determined for a specified extraparticle liquid-phase composition by first calculating the equilibrium hydrogen ion concentration in the adsorbed phase. This is done by substituting Eq. 29 solved for the adsorbed-phase protein concentration into the adsorbed-phase electroneutrality condition (Eq. 21) modified to include the proteins by extending the summation to include the quantity $z_{P_i,\text{ads}}C_{P_i}$ for all the proteins. As an approximation, $z_{P_i,\text{ads}}$ can be either equated to $z_{P_i,\text{fluid}}$ or determined by Eq. 27 with the pH in the adsorbent substituted for pH_{fluid}. In the former case the derivative needed in Newton's method for solving for $q_{H^+,\text{ads}}$ from the electroneutrality relation is given by Eq. 24, but with the following term added:

$$\sum_{i=1}^{N_P} z_{P_i,ix} z_{P_i,\text{ads}} K_{P_i} C_{P_i,\text{ads}} C_{H^+}^{-z_{P_i,\text{ads}}} (q_{H^+,\text{ads}})^{z_{P_i,\text{ads}}-1}, \quad (32)$$

while in the latter case the following terms are added:

$$\sum_{i=1}^{N_P} \left[z_{P_i,\text{ads}} z_{P_i,ix} + \frac{a_{i,\text{ref,fluid}} + 2b_{i,\text{ref,fluid}}[\text{pH}_{i,\text{ref,fluid}} + \log_{10}(q_{H^+})]}{\ln(10)} \right] \times K_{P_i,\text{ads}} C_{P_i} C_{H^+}^{-z_{P_i,ix}} (q_{H^+,\text{ads}})^{z_{P_i,ix}-1}. \quad (33)$$

As in the preceding section, the choice of which option to use will generally have to be determined experimentally. In any event, it is necessary to include the proteins in the electroneutrality condition only when their concentration is large. For dilute proteins, the equilibrium pH of the adsorbed phase can be determined without considering the proteins, and the amount of protein adsorbed can be determined explicitly from Eq. 29.

The method just described ignores the fact that adsorbed proteins prevent by steric interactions the adsorption of other proteins on adjacent surface sites (Brooks and Cramer, 1992). This effect, which becomes important at high protein concentrations, can be included here by suitable modification of Eq. 29. For simplicity, however, steric interactions will be ignored and it will be assumed that only a moderate amount of concentration overloading exists, where Eqs. 29 and 31 can usually fit the protein adsorption isotherms.

Transport Relations

If it is assumed that mass transfer occurs only in the pores of the adsorbent, then the mass-transfer rate is given by the Nernst-Planck equation as follows (Frey and Wong, 1989; Leaist and Lyons, 1981)

$$J_i = -D_{i,\text{eff}} \nabla C_i - \frac{z_i C_i D_{i,\text{eff}} F \nabla \phi}{RT} \quad (34)$$

where the subscript i denotes any of the ions present, and $D_{i,\text{eff}}$ is an effective diffusivity that includes the effects of particle porosity and tortuosity. If equilibrium exists between the pore fluid and the adjacent adsorbed phase in the pore, and if the ratio of the equilibrium concentrations of ion i in the entire particle and in the pore liquid at an average particle composition is denoted by Λ_i, then Eq. 34 can be written approximately as

$$J_i = -\frac{D_{i,\text{eff}}}{\Lambda_i} \nabla q_i + \frac{z_i q_i \dfrac{D_{i,\text{eff}}}{\Lambda_i} F \nabla \phi}{RT}. \quad (35)$$

If Eq. 35 is written for each ion, an expression for the total electric current can be developed which, when set equal to zero, can be used to eliminate the electric potential from Eq. 35. This results in relations of the following type

$$J_i = -\sum_{j=1}^{N_{\text{total}}} D_{ij,q} \nabla q_j \quad (36)$$

where

$$D_{ij,q} = \delta_{ij} \frac{D_{i,\text{eff}}}{\Lambda_i} - \frac{z_i z_j q_i (D_{i,\text{eff}}/\Lambda_i)(D_{j,\text{eff}}/\Lambda_j)}{\sum_{k=1}^{N_{\text{total}}} z_k^2 q_k \dfrac{D_{k,\text{eff}}}{\Lambda_k}} \quad (37)$$

and where N_{total} is the total number of species present, including the hydrogen and hydroxide ions. Equation 37 can be used to calculate the mass-transfer rate using any of the matrix approximations discussed by Wong and Frey (1989). The simplest procedure, which is exact for small mass-transfer driving forces, is to use the relation

$$R_{A_i^-} = -\sum_{j=1}^{N_{\text{total}}} \frac{60 D_{ij,q}}{d_p^2} (\bar{q}_j - \bar{q}_j^*) \quad (38)$$

where the overbars denote the average concentration in the particle. It should be noted that satisfying the condition of no electric current appears to be essential in order to accurately predict the effluent pH profile and that, for ion-exchange "resins" that have an ill-defined pore structure and where the entire particle constitutes the adsorbed phase, Eqs. 35–38 still apply, but with $D_{i,\text{eff}}/\Lambda_i$ replaced by $D_{i,q}$, that is, by the resin-phase diffusivity of ion i.

Material-Balance Relations and their Integration

If axial dispersion is ignored, the material-balance relation describing each buffering species can be written

$$\alpha \frac{\partial C_{A_i}}{\partial t} + \alpha v_{\text{fluid}} \frac{\partial C_{A_i}}{\partial x} + (1-\alpha) \frac{\partial \bar{q}_{A_i}}{\partial t} = 0 \quad (39)$$

where

$$\frac{\partial \bar{q}_{A_i}}{\partial t} \equiv R_{A_i} = R_{A_i^+} + R_{A_i^0} + R_{A_i^-}. \quad (40)$$

Equations 39 and 40, together with the equilibrium relations, can be solved numerically using the method of characteristics with a modified Euler integration method in Figure 3

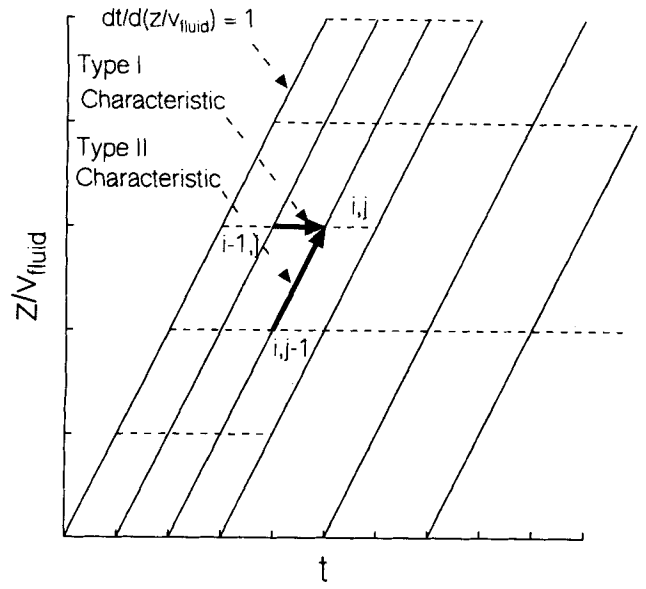

Figure 3. Characteristic directions for the method of characteristics.

(Acrivos, 1956; Loureiro and Rodrigues, 1991). To apply the method, the equations are integrated in two characteristic directions. Along the type I characteristics the following applies:

$$\left(\frac{d\bar{q}_{A_i}}{dt}\right)_I = R_{A_i}, \tag{41}$$

while the following applies along the type II characteristics:

$$\left(\frac{dC_{A_i}}{dx/v_{\text{fluid}}}\right)_{II} = -\frac{1-\alpha}{\alpha} R_{A_i}. \tag{42}$$

In the general case, the initial conditions in the adsorbent bed and the boundary conditions at the bed entrance are specified. To determine the concentrations at any interior point i,j (see Figure 3) Newton's method is first used to determine the individual ion concentrations in each phase from the total amounts of each buffering species in each phase at the points $i-1,j$ and $i,j-1$. The transport rates of each individual ion at the points $i-1,j$ and $i,j-1$ can then be determined using Eq. 38 and summed to yield the rate of interphase mass transfer for each buffering species at those locations. The quantities can then be used in Eqs. 41 and 42 to estimate the change in the concentrations of the buffering species (dC_{A_i} and $d\bar{q}_{A_i}$) along each characteristic using Euler's method. Next, those estimates are used to calculate in sequence the individual ion concentrations in both the liquid and adsorbed phases using Newton's method and the rates of interphase mass transfer at the point i,j. Finally, this estimate for R_{A_i} at the point i,j is used to recalculate the concentrations of the buffering species at i,j by making a second Euler integration step from the points $i-1,j$ and $i,j-1$ using an average value of R_{A_i} for the interval in question.

The efficiency of this procedure can be increased in several ways. First, an adjacent, previously solved point can be used to supply the starting guesses whenever Newton's method is employed to determine the individual ion concentrations. Second, the numerical integration is generally stable if $v_{\text{fluid}}dt/dx < 1$, in agreement with recognized stability criteria (Press et al., 1986). Since values for dt and dx must also be chosen to ensure accuracy, this implies that the time and distance grid spacing can often be increased as time proceeds, while keeping the ratio dt/dx constant, to account for the fact that the concentration gradients inside the column usually decrease in magnitude with time. Third, stepwise composition changes at the column entrance can be smoothed to prevent the occurrence of very large transport rates for the first distance grid point.

Comparisons with Measured Effluent pH Profiles

Although detailed experiments will be reported later, it is useful to include here sufficient experimental results to verify the accuracy of the theory just described. For the experiments performed here, 500-μm, strong-base, anion-exchange particles (Bio Rex MSZ1, Bio-Rad Laboratories) composed of 12% cross-linked styrene-divinylbenzene copolymer derivatized with quaternary amine groups were packed into a 1 cm × 17 cm column. A pump (Model RP-SY with a Model RH1CKC pump head, Fluid Metering) and pulse dampener (Model PD-60-LF) were used to deliver the solvent to the column. The pH in the column effluent was measured using a custom-fabricated sampling cell into which was inserted an Orion Model 91-03 pH minielectrode connected to an Orion Research Model 701A Ionalyzer. The buffers used were *N*-morpholinoethane sulfonic acid (MES, $pK_a = 6.1$) and *N*-morpholinopropane sulfonic acid (MOPS, $pK_a = 7.2$), which were obtained from Sigma and Boehringer Mannheim Gmbh, respectively.

Figure 4 shows theoretical calculations and experimental results for a column that was presaturated with a 50-mM NaOH solution titrated to pH 7.44 with MOPS, and eluted with a 50-mM NaOH solution titrated to pH 6.1 with MES. Note that the time axis in Figure 4 was nondimensionalized using the quantity L/v_{fluid}, which is denoted by t_0. The calculations assume that $K_{A_i^-,\text{ads}} = K_{A_i^\circ,\text{ads}} = 1$ for both buffering species so that $K_{\text{MES}^-\text{MOPS}^-,\text{ads}} = 1$, which is the expected value since MES and MOPS are structurally similar. According to Eqs. 22 and 23, this also implies $\Lambda_i = q_{\text{total}}/C_{\text{total}}$ for the anionic forms of MES and MOPS.

The first pH transition in the profile shown in Figure 4 is square-root broadening in nature (that is, its width is proportional to the square root of the distance traveled) since MES is absent in the transition so that the transition involves only changes in the concentration of MOPS. The position of this transition is determined mainly by the ratio $K_{\text{MOPS}^\circ,\text{ads}}/K_{\text{MOPS}^-,\text{ads}}$ and by the ion-exchange capacity of the adsorbent (q_R), while its shape (such as its width) is determined by the ratio $K_{\text{MOPS}^\circ,\text{ads}}/K_{\text{MOPS}^-,\text{ads}}$ and by the diffusion coefficients for MOPS^- and MOPS°. The second pH transition in Figure 4 is self-sharpening in nature since it involves the ion exchange of MES^- and MOPS^-. Its position is determined by q_R, while its shape is determined by the parameter $K_{\text{MES}^-,\text{MOPS}^-,\text{ads}}$ and by the diffusion coefficients of MES^- and MOPS^-. The diffusivities of H^+ and OH^- have only minor effects on the pH profile.

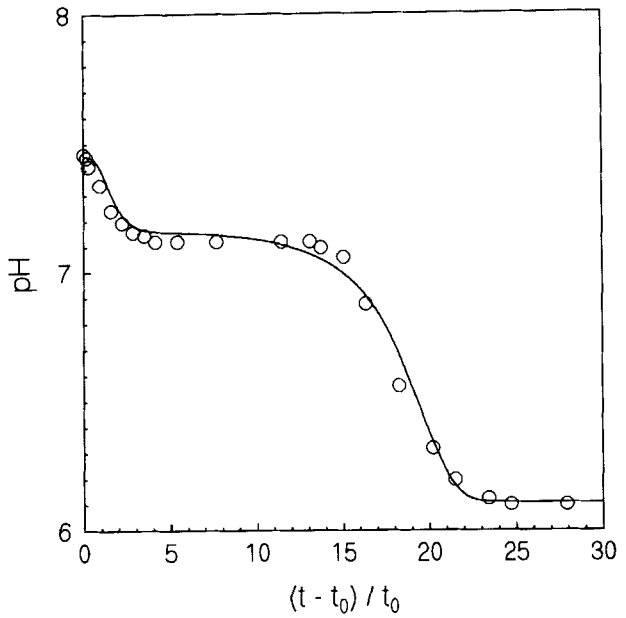

Figure 4. Experimental and calculated effluent pH profile for a chromatography column packed with a strongly basic anion-exchange adsorbent presaturated with *N*-morpholinopropane sulfonic acid ($pK_a = 7.2$) at pH 7.44 and eluted with *N*-morpholinoethane sulfonic acid ($pK_a = 6.1$) at pH 6.1.

Calculations correspond to $q_R = 0.95$ M, and to $D_{i,\text{eff}}/\Lambda_i = 3.35 \times 10^{-8}$ and $K_{A_i^-,\text{ads}} = K_{A_i^0,\text{ads}} = 1$ for both buffering species.

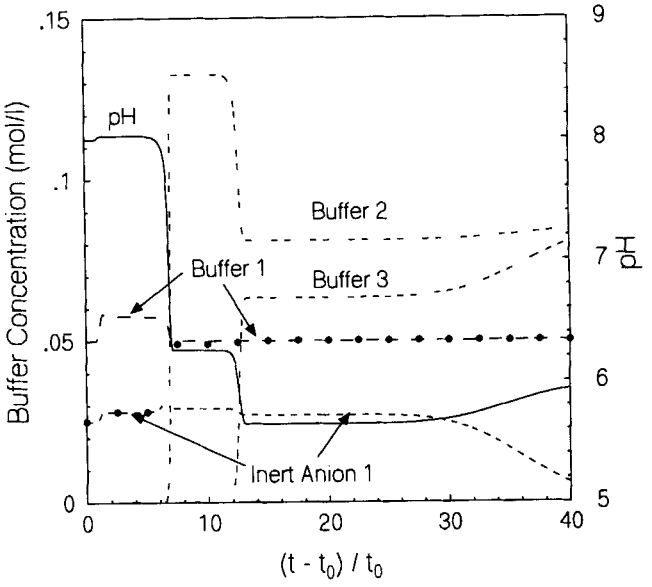

Figure 5. Effluent pH and buffering species concentration profiles for an adsorbent with equal amounts of strongly and weakly basic functional groups.

The column is initially in equilibrium with 0.05 M buffer 1 and 0.025 M anion 1 at pH 8. Feed conditions: 0.05 M buffer 1; 0.083 M buffer 2; 0.083 M buffer 3, pH 6. pK_a values and charges on the acidic form for buffers 1, 2, and 3 are 8.0, 7.0, 6.0 and 1, 0, 0, respectively. The total anion concentration is denoted by the solid circles.

In order to achieve the best fit to the data, the quantity D_i/Λ_i was set equal to 3.35×10^{-8} cm^2/s for each form of each buffering species, and to 3.8×10^{-7} and 2.2×10^{-7} cm^2/s, respectively, for H^+ and OH^-. Since Bio Rex MSZ1 is a typical ion-exchange resin in that it does not have well-defined pores, these quantities should be interpreted as diffusion coefficients in the adsorbed phase, that is, as $D_{i,q}$. These diffusivities are all approximately 4×10^{-3} times their values in aqueous solution and compare well with diffusion coefficients measured in related systems (Jones and Carta, 1993). The ion-exchange capacity used in the calculations was 30% less than the capacity for small ions measured by titrating the resin in the hydroxide form with dilute HCl. This also agrees with the results of Jones and Carta, who found that ion-exchange capacities decrease significantly with the size of the adsorbed ion. As shown in Figure 4, good agreement was achieved between experimental results and numerical calculations using these parameters.

Numerical Studies of pH Gradient Formation

Although the technique of chromatofocusing as typically practiced employs synthetic-polymer buffers composed of large numbers of buffering species, for clarity in the calculations shown here only the minimum number of buffering species needed to illustrate the effects under consideration will be used. In addition, as will be demonstrated, a small number of buffering species will be sufficient for many practical purposes. Furthermore, this work emphasizes the use of well-defined buffering species rather than synthetic polymer buffers. Since the most common types of amphoteric buffering species have functional groups with pK_a values sufficiently different that the titration of only one such group determines the ion-exchange behavior, it will be assumed that all buffering species are monofunctional weak electrolytes. Finally, since good agreement between theory and experiments was achieved in Figure 4 where only monovalent ions were present, it will also be assumed in the following calculations that $K_{A_i^-,\text{ads}} = K_{A_i^0,\text{ads}} = 1$ for every buffering species so that $K_{A_j^-A_i^-,\text{ads}} = 1$ for all the exchanging ions. These simplifications imply that the simulations presented here are somewhat idealized and primarily serve to illustrate the general behavior of chromatography systems employing pH gradients. More realistic systems will be investigated in future studies in conjunction with detailed experimental results.

Figure 5 illustrates effluent pH and concentration profiles produced under conditions generally employed in chromatofocusing on anion-exchange adsorbents (Hutchens et al., 1986a,b; Pharmacia, 1980). In particular, the column is presaturated at pH 8 with a mixture of a strong acid (that is, an acid that produces inert anion 1) and a buffering species whose pK_a is near the presaturation pH value and whose acidic form is a cation (that is, buffer 1, whose pK_a is 8). The eluent pH is 6 and is composed of a mixture of buffering species whose pK_a values span the pH range of interest. This mixture contains the same buffering species used to presaturate the column along with two other buffering species having lower pK_a values and whose acidic forms are uncharged,

Table 1. Physical Properties Used in Numerical Calculations

Symbol*	Value
$a_{i,ix}$	1.5
$a_{i,\text{fluid}}$	4.0
$b_{i,ix}$	0.0
$D_{A,\text{eff}}$	1×10^{-6} cm^2/s
$D_{P,\text{eff}}$	2×10^{-7} cm^2/s
$D_{\text{H}^+,\text{eff}}$	9×10^{-6} cm^2/s
$D_{\text{OH}^-,\text{eff}}$	5×10^{-6} cm^2/s
d_p	100 μm
$K_{A,\text{ads}}$	1.0
$K_{P,\text{ads}}$	1.0
L	10 cm
q_R	1 M
v_{fluid}	0.1 cm/s
α	0.35
β	1.0

*The symbol A denotes any of the charged forms of A_i.

that is, buffers 2 and 3, whose pK_a values are 7 and 6, respectively.

The pK_a values for the functional groups attached to the adsorbent in the calculations shown in Figure 5 were chosen so that the adsorbent behaves like those commonly used in chromatofocusing, such as the specialized forms of polyethyleneimine-derivatized agarose manufactured by Pharmacia (1980). More specifically, an anion exchanger was employed that has equal amounts of two types of functional groups: a strongly basic group that is always positively charged and a weakly basic group whose pK_a is 8.25 so that it is nearly uncharged when the liquid-phase pH is 8 (in which case the adsorbed-phase pH is 9.3) and is nearly fully charged when the liquid-phase pH is 6 (in which case the adsorbed-phase pH is 7.3). A particle diameter of 100 μm was employed, which is typical for process-scale chromatography, and the effective diffusion coefficient in the pores for all the charged forms of each buffering species was 10^{-6} cm^2/s. As discussed earlier, $K_{A_i^-,\text{ads}}$ and $K_{A_i^0,\text{ads}}$ were set equal to unity for all ions, and the presence of unadsorbed material in the particle pores was ignored, that is, $\beta = 1$ was assumed for the purpose of determining adsorption equilibrium. Other parameters are summarized in Table 1 and the figure caption.

Figure 5 shows that, for the conditions just described, there is a small pH increase at the start of the elution step due to the behavior of buffer 1. In particular, there is a significant amount of the unchanged form of buffer 1 initially in the adsorbent. The pK_a of buffer 1 is sufficiently large, however, so that a substantial decrease in pH converts all of buffer 1 to the positively charged form, which is weakly adsorbed. After this initial pH increase, there is a pH decrease in a series of two self-sharpening transitions to a pH plateau below the eluent pH. These self-sharpening transitions are caused by the adsorption of buffers 2 and 3 and have velocities that satisfy Eq. 2 written for the plateau concentrations of any of the buffering species or for the plateau concentrations of inert anion 1. Since the concentration of inert anion 1 changes by only a small amount in these two transitions, Eq. 2 indicates that the adsorbed-phase concentration of inert anion 1 must also change by only a small amount. This implies that the increase in adsorbed concentrations of buffers 2 and 3 during the two transitions is nearly equal to the increase in adsorbent ion-exchange capacity.

In the final portion of the effluent profile in Figure 5 there is a gradual increase in pH to the value for the eluent. Figure 5 also shows that the total ionic concentration in the effluent does not remain constant. Instead, it is largely determined by the fraction of buffer 1 that is ionized since that buffering species is the only one that forms a cation and it is never adsorbed in large amounts. This shows that when an anion-exchange adsorbent is employed, buffering species can be selected for the eluent that are positively charged in their acidic form, and that have pK_a values between the presaturation and elution pH values, so that the titration of these buffering species causes the liquid-phase total ionic concentration to increase during a particular pH transition. Furthermore, since the total ionic concentration increases when the pH decreases, this effect can be used to assist in protein desorption.

The results shown in Figure 5 can be compared to experimental data reported in the literature, for example, that of Hutchens et al. (1986a,b), who used as an eluent a multicomponent mixture of buffering species including 2-amino-2-hydroxymethyl-1,3-propanediol (TRIS) having a pK_a of 8.06; *N*-(2-acetamido)-2-aminoethane sulfonic acid (ACES) having a pK_a of 6.9; and MES, having a pK_a of 6.15, which correspond closely to the properties of buffers 1, 2, and 3, respectively. For example, Figure 4 of Hutchens et al. (1986a) as well as Figure 4 of Hutchens et al. (1986b) show results using a polyethyleneimine-silica adsorbent possessing roughly equal portions of strongly and weakly basic functional groups together with a TRIS buffer at pH 8 as the presaturant and the multicomponent buffer mixture just described as the eluent. All of the features just mentioned were observed for this system, including a small increase in pH above the presaturation value at the start of the elution step and a decrease to a pH of approximately a 0.5 unit below the eluent pH near the end of the elution step. As shown in Figure 6, similar features are also observed for commercially available chromatofocusing systems (see also Pharmacia, 1980, Figures 18 and 22). Note that in Figure 6 the elution step was terminated before the column became equilibrated with the eluent.

As just mentioned, for the buffer system used in Figure 5 an increasing ion-exchange capacity with a decreasing pH is required to produce a series of pH steps corresponding to the adsorption of buffering species in the eluent. Several experimental studies have also indicated that an adsorbent with a buffering capacity in the pH range of interest is required to achieve a controlled pH gradient (Pharmacia, 1980). This conclusion is also consistent with the calculations in Figure 7, which illustrates the effluent pH and concentration profiles for the same eluent and presaturation conditions as in Figure 5, but with an adsorbent having a fixed ion-exchange capacity. As shown, after an initial pH fluctuation, the concentration of inert anion 1 in both the liquid and adsorbed phases is again nearly constant as the pH decreases from the presaturation value. However, since the ion-exchange capacity is fixed, there must also be a small change in both the adsorbed- and liquid-phase concentrations of the negatively charged forms of buffers 2 and 3 during the transition. This is accomplished by having a large pH decrease during the transition so that, although the liquid-phase concentrations of those two buffering species are significant on the upstream side of the transition, the liquid-phase concentrations of the

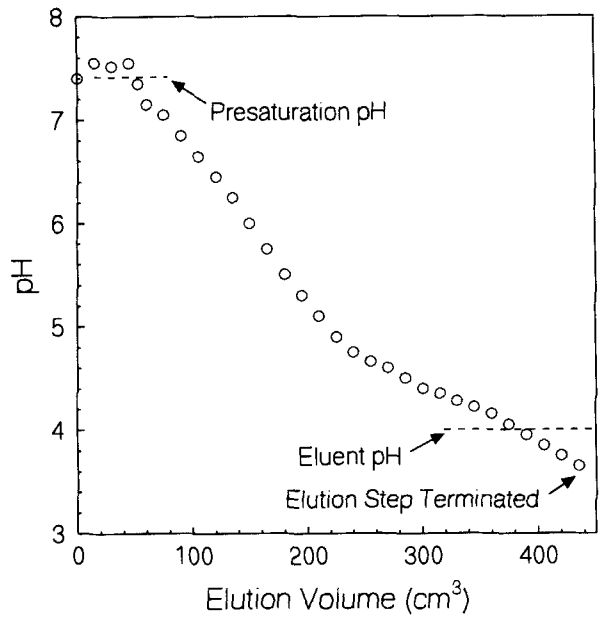

Figure 6. Effluent pH profile for a column of PBE 94 (Pharmacia) presaturated with 0.025 M imidazole adjusted with HCl to pH 7.4 and eluted with polybuffer 74 (Pharmacia) diluted 1:8 and adjusted to pH 4 with HCl (Matthews and Walsh, 1987).

negatively charged forms of those buffering species are small on that side.

Although the buffer system in Figure 5 represents those

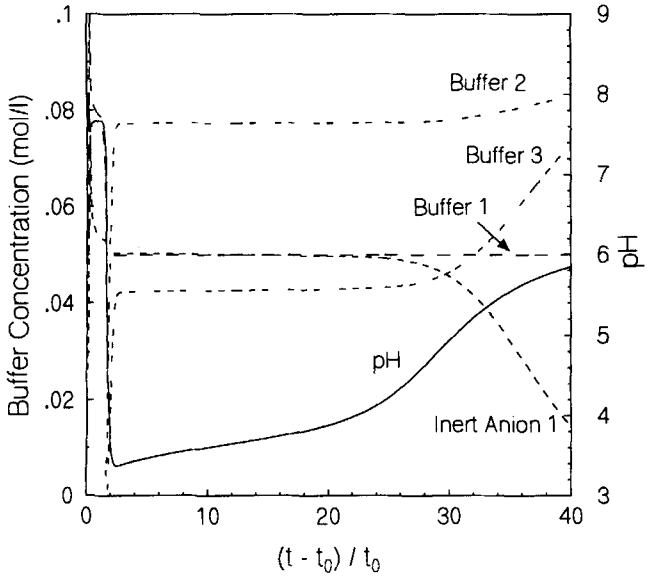

Figure 7. Effluent pH and buffering species concentration profiles for an adsorbent with only strongly basic functional groups.

The column is initially in equilibrium with 0.05 M buffer 1 and 0.025 M anion 1 at pH 8. Feed conditions: 0.05 M buffer 1; 0.083 M buffer 2; 0.083 M buffer 3, pH 6. pK_a values and charges on the acidic form for buffers 1, 2, and 3 are 8.0, 7.0, and 6.0 and 1, 0, 0, respectively.

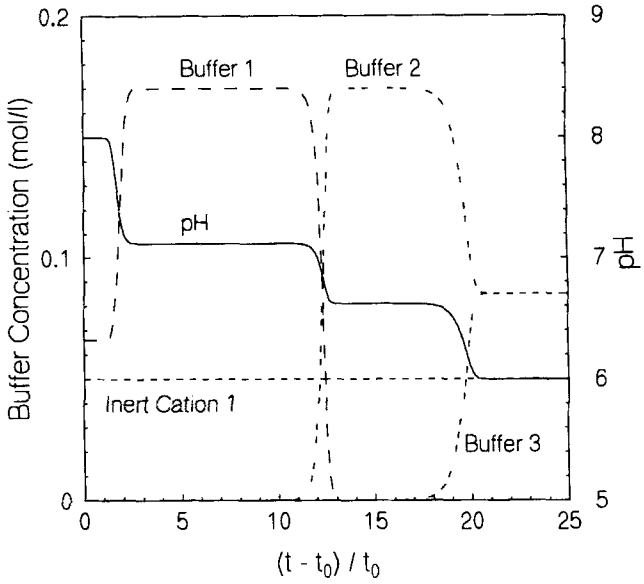

Figure 8. Effluent pH and buffering species concentration profiles for an adsorbent with only strongly basic functional groups.

The column is initially in equilibrium with 0.05 M cation 1 and 0.066 M buffer 1 at pH 8.0. Feed conditions: 0.05 M cation 1; 0.083 M buffer 2; 0.083 M buffer 3, pH 6. pK_a values and charges on the acid form for buffers 1, 2, and 3 are 7.5, 7.0, 6.0, and 0, 0, 0, respectively. The total anion concentration is equal to the concentration of cation 1.

widely employed in chromatofocusing, Figures 8 and 9 illustrate an alternative buffer system, similar to that used for the experiments in Figure 4, which has several advantages. For the calculation shown, all of the buffering species are unchanged in their acidic form. The column is again presaturated at pH 8 with the buffering species having the highest pK_a, that is, buffer 1, which has a pK_a of 7.5 and an anionic form that is adsorbed at the presaturation pH. Finally, the only cations present are inert in the sense that they are conjugate bases of strong acids so that they do not participate in acid-base equilibrium. This buffer system is similar to that used in the studies by Sluyterman and Wijdenes (1978).

Figure 8 illustrates the effluent pH and concentration profiles for the buffer system just described, and for an adsorbent that has only strongly basic functional groups and therefore a fixed adsorption capacity, while in Figure 9 the same buffer system is used but with an adsorbent that has equal amounts of strongly and weakly basic functional groups and therefore an adsorption capacity that varies with pH. A comparison of the figures indicates that presaturating the adsorbent with the anionic form of the buffering species with the highest pK_a value makes it possible to produce a pH profile that decreases in a series of well-defined steps even though the adsorbent does not contain weakly basic functional groups. Furthermore, when the column is presaturated as just stated, the effluent pH no longer decreases below the eluent pH as in Figure 5. This behavior, which is consistent with the results in Figure 4, is due to the fact that the anion that is initially adsorbed onto the column is removed in the first two pH transitions. These observations also agree with the work of Murel et al. (1986), who investigated related

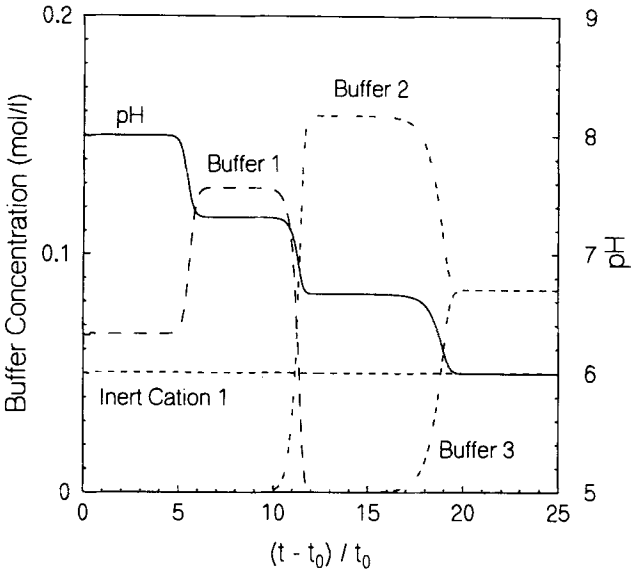

Figure 9. Effluent pH and buffering species concentration profiles for an adsorbent with equal amounts of one weakly ($pK_a = 8.25$) and one strongly basic functional group.

The column is initially in equilibrium with 0.05 M cation 1 and 0.066 M buffer 1 at pH 8; feed conditions: 0.05 M cation 1; 0.083 M buffer 2; 0.083 M buffer 3, pH 6. pK_a values and charges on the acidic form for buffers 1, 2, and 3 are 7.5, 7.0, 6.0 and 0, 0, 0, respectively.

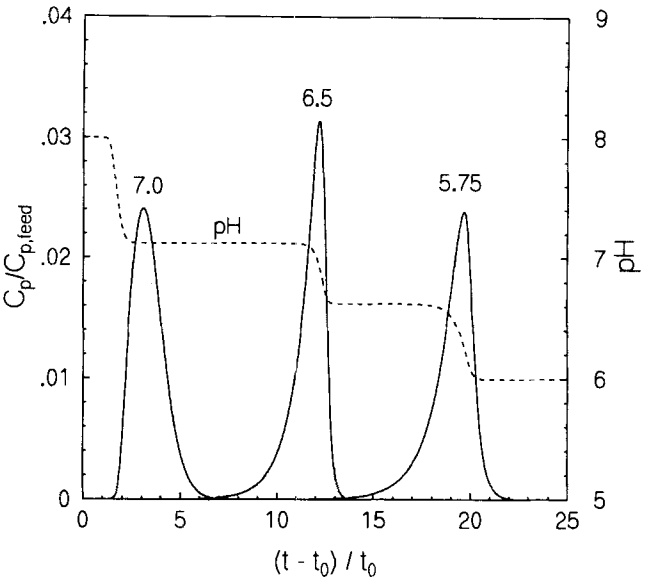

Figure 10. Simulated separation of proteins introduced in trace amounts using the same conditions as in Figure 7.

Protein feed concentration was 10^{-6} M. Numbers above the protein bands denote the isoelectric point.

methods for producing pH gradients using strong-base ion-exchange adsorbents.

It should be emphasized that strong-base ion-exchange adsorbents have several practical advantages for protein separations as compared to the specialized, weak-base adsorbents now commonly employed in chromatofocusing. These advantages include the fact that strong-base adsorbents tend to be less expensive, to have a higher protein adsorption selectivity due to their higher surface charge density, to have a higher protein adsorption capacity, to have a higher lot-to-lot consistency in adsorbent properties, and to be available in a wider variety of forms so that adsorbents with enhanced mechanical and chemical stability or superior mass-transfer properties can be employed. For these reasons, the adsorbent-buffer system shown in Figure 8 is likely to be a practical alternative to systems currently used for chromatofocusing.

Numerical Studies of Protein Separation

In this section numerical calculations are employed to investigate protein separations using internally generated pH gradients. Figure 10 depicts the separation of three proteins introduced into the column at dilute concentration in a small feed slug and using the same adsorbent-buffer system employed in Figure 8. Physical properties were chosen to be typical of small proteins, that is, a value of 2×10^{-7} cm^2/s was employed for the effective diffusivity in the particle pores. The parameter $b_{i,ix}$ was set equal to zero and the value of $a_{i,ix}$ used was 1.5 pH^{-1}, which is an average of the values obtained by Hearn et al. (1987) for four different proteins. Other parameters are given in Table 1. As was the case in Figure 4, the first pH transition in Figure 10 is square-root broadening in nature, while the second and third transitions are self-sharpening.

As shown in Figure 10, the three proteins are readily separated under the conditions shown. In addition, it can be seen that the presence of self-sharpening pH transitions is beneficial since these transitions are comparatively steep and therefore are able to concentrate as well as separate proteins through a focusing effect even though the protein mass-transfer efficiency is relatively low. Figure 10 also shows that protein bands that elute later in time are located on the pH gradient farther from their isoelectric points as compared to protein bands that elute earlier in time. In particular, the three proteins shown have isoelectric points of 7.0, 6.5 and 5.75 and have band centers located on the pH gradient 0.1, 0.4, and 0.7 pH units higher than their isoelectric points, respectively. This behavior is due to the fact that proteins must be more highly charged, and hence farther from their isoelectric pH, to become more strongly retained by the column. This behavior also agrees with the observations of Sluyterman and Wijdenes (1978), who observed protein bands eluting at a position on the pH gradient up to one pH unit away from their isoelectric point. The net effect is that the two bands farthest upstream satisfy the focusing criterion described by Eq. 2, and are therefore positioned on steep pH transitions where a focusing effect leads to relatively narrow bands. In contrast, the first protein band is located on a pH plateau and is comparatively broad.

Figures 11 and 12 illustrate the effect of volume overloading, and a combination of volume and concentration overloading, respectively. Both figures employ the same conditions used in Figure 10 except that a feed slug width of 10 t_0 was employed, which is 40% of the total elution time. In keeping with the use of Eqs. 29 and 37 for describing the protein adsorption and diffusional behavior, however, only a

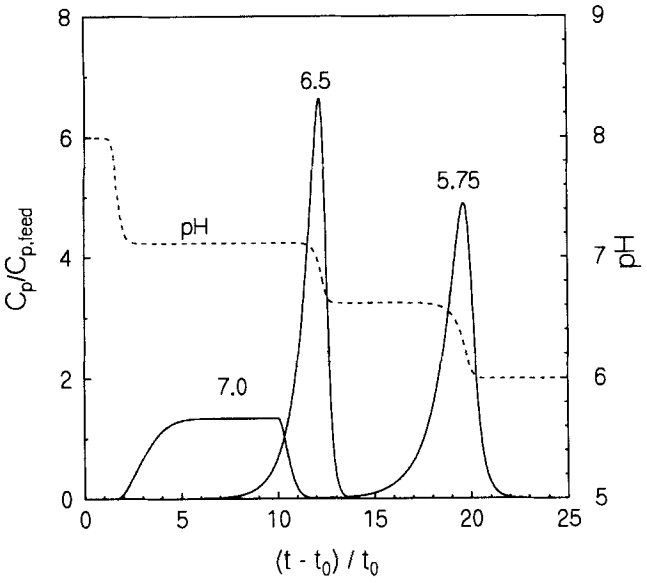

Figure 11. Simulated separation of proteins under volume overloaded conditions.

Feed slug size was 10 t_0 and protein feed concentration was 10^{-6} M. Numbers above the protein bands denote the isoelectric point.

modest amount of concentration overloading was employed in Figure 12. As shown, despite the severe amount of volume overloading, and despite the relatively large particle size used, the protein bands are still well resolved. In particular, the two bands that are primarily located on a pH transition, and that are therefore subject to strong focusing effects, have widths similar to those in Figure 10. In contrast, the first protein band, which is still located primarily on a pH plateau, is nearly as broad as the feed slug. Figures 11 and 12 also indicate that concentration overloading leads to broader bands and a somewhat degraded separation. This is because the presence of proteins at high concentration in a pH transition causes the transition to become more shallow. This is most apparent for the protein band farthest upstream in Figures 11 and 12 since that band is located on the pH gradient farthest from its isoelectric point so that it has the largest net charge of the three proteins shown.

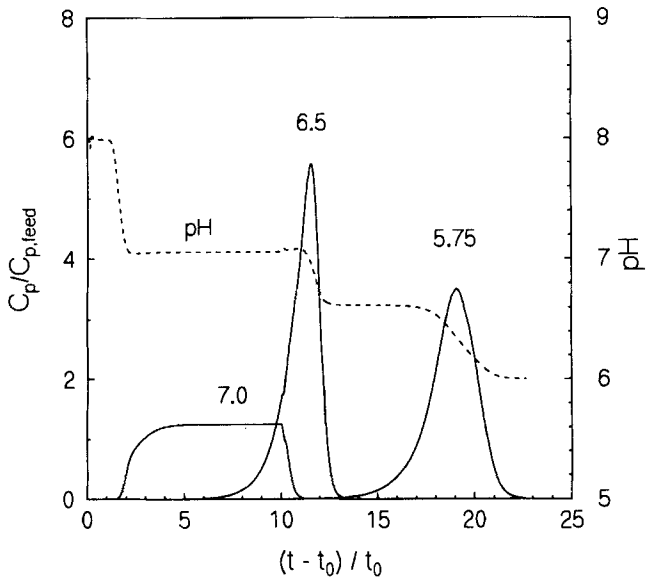

Figure 12. Simulated separation of proteins under volume and concentration overloaded conditions.

Feed slug size was 10 t_0 and protein feed concentration was 10^{-3} M. Numbers above the protein bands denote the isoelectric point.

The calculations in Figures 11 and 12 indicate that it is practical to develop preparative chromatography processes using limited numbers of buffering species so that a protein band is confined to either a pH transition or plateau as desired. In this regard, Figures 11 and 12 illustrate a practical goal when using internally produced pH gradients. Namely, since proteins tend to have limited solubilities near their isoelectric point, the early eluting protein bands should be located on a pH plateau where the focusing effect is weak since they are positioned on the pH profile near their isoelectric point. In contrast, protein bands that are eluted later in time, and that tend to be positioned on the pH profile farther away from their isoelectric point, should be located on a steep pH transition where a strong focusing effect leads to narrow bands with a high average protein concentration.

Conclusions

A general numerical method based on the method of characteristics is developed for chromatography employing pH gradients under conditions where several buffering species are adsorbed onto the stationary phase. The method is able to predict the detailed behavior of such systems, such as the shape of the pH gradient, the location of protein bands relative to their isoelectric point, and the variation in liquid-phase total ion concentration. In contrast to widely recommended operating procedures, it is shown that it is not necessary in chromatographic processes such as chromatofocusing that employ retained pH gradients to use an adsorbent with a buffering capacity provided that the column is presaturated with an adsorbed buffering ion having a pK_a value near the presaturation pH. Such a presaturation condition also ensures that a monotonically decreasing pH gradient is achieved. It is also shown that a properly designed preparative chromatography system can produce either highly concentrated proteins or proteins near their concentration in the feed slug, depending on the choice of buffering species.

Acknowledgments

Support from the Donors of the Petroleum Research Fund and from grant CTS 9008746 from the National Science Foundation is gratefully acknowledged.

Notation

a_i, b_i = fitting parameters, pH^{-1} and pH^{-2}
A, B = buffering species (e.g., A_i) or any charged form of a buffering species (e.g., A_i^-), according to context
C_A = concentration in liquid phase, mol·cm^3
D_A = diffusion coefficient, cm^2·s^{-1}
d_p = particle diameter, cm
F = Faraday constant, 96,487 C·equiv^{-1}
$K_{A,ads}$ = adsorption equilibrium constant for buffering species
$K_{AB,ads}$ = exchange equilibrium constant for buffering species

$K_{A,\text{fluid},1}$ = first liquid-phase dissociation constant for buffering species, mol·cm^{-3}
$K_{A,\text{fluid},2}$ = second liquid-phase dissociation constant for buffering species, mol·cm^{-3}
$K_{P,\text{ads}}$ = adsorption equilibrium constant for protein
$K_{R,1}$ = first dissociation constant for adsorbent functional group, mol·cm^{-3}
$K_{R,2}$ = second dissociation constant for adsorbent functional group, mol·cm^{-3}
$K_{w,\text{ads}}$ = dissociation constant for water in adsorbent, mol^2·cm^{-6}
$K_{w,\text{fluid}}$ = dissociation constant for water in liquid phase, mol^2·cm^{-6}
N_A = number of buffering species
N_P = number of proteins
N_R = number of functional group types attached to adsorbent
q_A = concentration per unit volume of particle, mol·cm^{-3}
$q_{A,\text{ads}}$ = concentration per unit volume of adsorbed phase, mol·cm^{-3}
R_i = ion exchange functional group attached to adsorbent
R_A = adsorption rate of A per unit volume of particle, mol·cm^{-3}
t = time, s
$t_0 = L/v_{\text{fluid}}$, s
v_p = velocity of a protein concentration level, cm·s^{-1}
v_{fluid} = interstitial velocity of fluid, cm·s^{-1}
v_i = velocity of a concentration level of component i, cm·s^{-1}
x = axial distance down column, cm
z = ionic charge

Greek letters

α = void volume in bed
β = volume fraction of adsorbed phase in sorbent
δ_{ij} = Kronecker delta function
ϵ = internal porosity of particle
Λ_A = ratio of concentrations of a component in the adsorbed and liquid phases at equilibrium
ρ_b = bulk density of particle, g·cm^{-3}

Superscript and Subscript

+, −, o = charge type
* = value in equilibrium with contacting phase
ads = adsorbed phase
A_i = buffering species
d = downstream from composition change
eff = effective value
fluid = liquid phase
i = component i
ix = related to ion-exchange mechanism
m = solvent modifier
P_i = protein
q = quantity based on particle phase concentration driving force
ref = reference value used in charge calculation
total = value corresponding to total equivalent concentration
u = upstream from composition change

Literature Cited

Acrivos, A., "Method of Characteristics Technique," *Ind. Eng. Chem.*, **48**, 703 (1956).

Berninger, J. A., R. D. Whitley, X. Zhang, and N.-H. L. Wang, "A Versatile Model for Simulation of Reaction and Nonequilibrium Dynamics in Multicomponent Fixed-Bed Adsorption Processes," *Comput. Chem. Eng.*, **15**(11), 749 (1991).

Brooks, C. A., and S. M. Cramer, "Steric Mass-Action Ion Exchange: Displacement Profiles and Induced Salt Gradients," *AIChE J.*, **38**, 1853 (1992).

Engasser, J.-M., and Cs. Horváth, "Buffer Facilitated Proton Transport: pH Profile of Bound Enzymes," *Biochim. Biophys. Acta*, **358**, 178 (1974).

Frey, D. D., and T. Wong, "General Linearized Matrix Theory of Electrochemical Mass Transfer with Applications to Electrode Processes and Ion Exchange," *Chem. Eng. Commun.*, **75**, 195 (1989).

Hearn, T. W., A. N. Hodder, P. G. Stanton, and M. I. Aguilar, "High-Performance Liquid Chromatography of Amino Acids, Peptides, and Proteins," *Chromatographia*, **24**, 769 (1987).

Helfferich, F. G., and B. Bennett, "Weak Electrolytes, Polybasic Acids, and Buffers in Anion Exchange Columns. 1. Sodium Acetate and Sodium Carbonate," *Solvent Extr. Ion Exch.*, **2**(7–8), 1151 (1984a).

Helfferich, F. G., and B. Bennett, "Weak Electrolytes, Polybasic Acids, and Buffers in Anion Exchange Columns: 2. Sodium Acetate and Sodium Chloride," *React. Polym., Ion Exch., Sorbents*, **3**(1), 51 (1984b).

Hutchens, T. W., C. M. Li, and P. K. Besch, "Performance Evaluation of a Focusing Buffer Developed for Chromatofocusing on High-Performance Anion-Exchange Columns," *J. Chromatog.*, **359**, 169 (1986a).

Hutchens, T. W., C. M. Li, and P. K. Besch, "Development of Focusing Buffer Systems for Generation of Wide-Range pH Gradients During High-Performance Chromatofocusing," *J. Chromatog.*, **359**, 157 (1986b).

Jones, I. L., and G. Carta, "Ion Exchange of Amino Acids and Dipeptides on Cation Resins with Varying Degrees of Cross-Linking," *Ind. Eng. Chem. Res.*, **32**, 107 (1993).

Klein, G., J. Sinkovic, and T. Vermeulen, "Weak-Electrolyte Ion Exchange in Advanced-Technology Water-Reuse Systems," U.S. Dept. of Interior Report No. OWRT/RU-82/7 (1982).

Leaist, D. G., and P. A. Lyons, "Multicomponent Diffusion of Electrolytes with Incomplete Dissociation. Diffusion in a Buffer Solution," *J. Phys. Chem.*, **85**, 1756 (1981).

Loureiro, J. M., and A. Rodrigues, "Two Solution Methods for Hyperbolic Systems of Partial Differential Equations in Chemical Engineering," *Chem. Eng. Sci.*, **46**, 3259 (1991).

Matthews, J. A., and D. J. Walsh, "Rapid Purification of a Major Allergen from Pollen of Cocksfoot Grass (Dactylis glomerata)," *Trans. London Biochem. Soc.*, **15**, 706 (1987).

Murel, A., S. Vilde, M. Pank, I. Shevchuk, and O. Kirret, "Chromatophoresis: A New Approach to the Theory and Practice of Chromatofocusing: I. General Principles," *J. Chromatog.*, **347**, 325 (1985).

Murel, A., S. Vilde, M. Pank, I. Shevchuk, and O. Kirret, "Chromatophoresis: A New Approach to the Theory and Practice of Chromatofocusing, II. Experimental Verification," *J. Chromatog.*, **362**, 101 (1986).

Press, W. H., B. P. Flannery, S. A. Teukolsky, and W. T. Vetterling, *Numerical Recipes: The Art of Scientific Computing*, Cambridge Univ. Press, Cambridge, England (1986).

Pharmacia Biotech AB Publications, *Chromatofocusing with Polybuffer and PBE*, Uppsala, Sweden (1980).

Saunders, M. S., J. B. Vierow, and G. Carta, "Uptake of Phenylalanine and Tyrosine by a Strong-Acid Cation Exchanger," *AIChE J.*, **35**(1), 53 (1989).

Saville, D. A., and O. A. Palusinski, "Theory of Electrophoretic Separations: Part 1. Formulation of Mathematical Model," *AIChE J.*, **32**, 207 (1986).

Scopes, R. K., *Protein Purification: Principles and Practice*, 2nd ed., Springer-Verlag, New York (1987).

Sluyterman, L. A. AE., and O. Elgersma, "Chromatofocusing: Isoelectric Focusing on Ion-Exchange Columns, I. General Principles," *J. Chromatog.*, **150**, 17 (1978).

Sluyterman, L. A. AE., and J. Wijdeness, "Chromatofocusing: Isoelectric Focusing on Ion-Exchange Columns: II. Experimental Verification," *J. Chromatog.*, **150**, 31 (1978).

Tanford, C., *Physical Chemistry of Macromolecules*, Wiley, New York (1960).

Wankat, P. C., *Large Scale Adsorption and Chromatography*, CRC Press, Boca Raton, FL (1986).

Wankat, P. C., *Rate-Controlled Separations*, Elsevier Applied Science, New York (1990).

Wong, T., and D. D. Frey, "Matrix Calculation of Multicomponent Transient Diffusion in Porous Sorbents," *Int. J. Heat Mass Transf.*, **32**(11), 2179 (1989).

Manuscript received Oct. 15, 1993, and revision received June 30, 1994.